Mon. Not. R. Astron. Soc. **281**, 1315–1325 (1996)

Line profile variations in γ Doradus

L. A. Balona,[1] T. Böhm,[2] B. H. Foing,[3] K. K. Ghosh,[4] E. Janot-Pacheco,[5] K. Krisciunas,[6] A.-M. Lagrange,[7] W. A. Lawson,[8] S. D. James,[8] J. Baudrand,[9] C. Catala,[10] M. Dreux,[10] P. Felenbok[10] and J. B. Hearnshaw[11]

[1]*South African Astronomical Observatory, PO Box 9, Observatory 7935, Cape, South Africa*
[2]*ESO, Karl-Schwarzschildstr. 2, D-85748, Garching, Germany*
[3]*Solar System Division, Space Science Department of ESA, ESTEC, The Netherlands*
[4]*Vainu Bappu Observatory, Indian Institute of Astrophysics, Kavalur, Alangayam, TN 635701, India*
[5]*Departamento de Astronomia, Instituto Astronomico e Geofisico da USP, C. Postal 9638, 01065-970 Sao Paulo, Brazil*
[6]*Joint Astronomy Centre, 660 N. A'ohōkū Place, University Park, Hilo, Hawaii 96720, USA*
[7]*Lab. Astrophys. Grenoble UJF, BP53X F, 38041 Grenoble Cedex, France*
[8]*School of Physics, University College UNSW, Australian Defence Force Academy, Canberra, ACT 2600, Australia*
[9]*Dep. Astrophys. Extragal. et de Cosmologie, Obs. de Paris, Section de Meudon, F-92195 Meudon Principal Cedex, France*
[10]*Obs. Midi-Pyrenees, 14 avenue Edouard Belin, 31400 Toulouse, France*
[11]*Mount John University Observatory, Department of Physics and Astronomy, University of Canterbury, Christchurch, New Zealand*

Accepted 1996 March 10. Received 1996 February 19; in original form 1995 December 29

ABSTRACT

We present data from high-dispersion echelle spectra and simultaneous *uvby* photometry for γ Doradus. These data were obtained from several sites during 1994 November as part of the MUSICOS-94 campaign. The star has two closely spaced periods of about 0.75 d and is the brightest member of a new class of variable early F-type stars. A previously suspected third period, very close to the other two, is confirmed. Previous observations indicated that sudden changes could be expected in the spectrum, but none was found during the campaign. The radial velocities rule out the possibility of a close companion. The phasing between the radial velocity and light curve of the strongest periodic component rules out the starspot model. The only viable mechanism for understanding the variability is non-radial pulsation. We used the method of moments to identify the modes of pulsation of the three periodic components. These appear to be sectorial retrograde modes with spherical harmonic degrees, (ℓ, m), as follows: $f_1 = (3,3)$, $f_2 = (1,1)$ and $f_4 = (1,1)$. The angle of inclination of the star is found to be $i \approx 70°$.

Key words: stars: individual: γ Dor – stars: oscillations – stars: variables: other.

1 INTRODUCTION

γ Doradus (F0V) is the brightest member of what appears to be a new class of pulsating variable stars. In recent years, a number of late A- and early F-type dwarfs have been found to be variable with periods of the order of one day (see Krisciunas & Handler 1995 for a list). This is too long for membership of the δ Scuti class, where the periods are just a few hours. The period is, in many cases, compatible with that expected for rotation, which suggests that the variability may be due to the rotation of a spotted star (Mantegazza, Poretti & Zerbi 1994). However, most stars appear to be multiperiodic and require improbably large differential rotation. The starspot model for γ Dor has been examined by Balona, Krisciunas & Cousins (1994b) who find that large overlapping spots would be required to give the observed light and colour amplitudes.

The most likely explanation for the variability in these stars is non-radial pulsation (NRP), since it is difficult to understand multiple periodicities in terms of the starspot model or as orbital motion. Multiple periods are typical of NRP, but one needs to prove that the physical parameters determined from an NRP model are realistic and that the other models are unable to explain the observations. In NRP, the light variability is due to the periodic variation in temperature and, to a smaller extent, the change in the shape of the star during pulsation. Pulsation with a period of about one day implies that the dominant restoring force is gravity (g modes), rather than pressure (p modes) as in the case of the δ Sct stars. Furthermore, because the stars show substantial light and radial velocity variations, the averaging effect over the visible hemisphere of the star must be quite small. This implies that the spherical harmonic degree, ℓ, of the pulsation must be

low, probably $\ell < 4$. Aerts & Krisciunas (1996) have analysed 9 Aur, a star belonging to this group, using photometry and the cross-correlation profile obtained with the CORAVEL instrument. They deduce that 9 Aur is pulsating in two modes, both having spherical harmonic indices $(\ell, m) = (3, |1|)$.

The mechanism that excites the pulsation is not known at present. The stars appear to be located at, or near, the red edge of the δ Sct instability strip. This indicates that the mechanism may be the same as for δ Sct stars (the ionization of H and He), but perhaps modified by convection.

It would certainly be interesting to examine the line profile and light variations of these stars. These data may enable us to distinguish between NRP and rotational modulation of a spotted star. NRP produces line profile and light variations which, in principle, allow the determination of the spherical harmonic degree, ℓ, and the azimuthal number, m. This can be done by examining the variation of the moments of a line profile and calculating a discriminant. The value of the discriminant as a function of angle of inclination is used to determine the most probable mode (ℓ, m). The method was developed by Balona (1986a,b, 1987) and extended by Aerts (1993).

The two periods of γ Dor are stable and well determined from extensive photometric observations: $P_1 = 0.757\,01$ d, $P_2 = 0.733\,39$ d (Balona et al. 1994a). More recently, evidence has been found for a third period at $P_4 = 0.677\,97$ d (Balona et al. 1994b). (We call this period P_4 and not P_3 because P_3 was used in Balona et al. (1994a) to refer to a possible single period, later shown to be incorrect.) Since the star is bright ($V = 4.3$) and well placed, it was chosen as one of the targets for the MUSICOS-94 programme. The aim was to obtain a large number of high signal-to-noise ratio line profiles which, in conjunction with Strömgren photometry, would decide which of the two models, starspots or NRP, is the correct one and to determine the spot geometry or pulsation modes. Another factor in choosing to observe this star is the rapid change in the spectrum which appears from time to time (Balona et al. 1994a). γ Dor is an *IRAS* source with a probable circumstellar dust cloud (Aumann 1985), which may be responsible for this effect.

In this paper we present details of the observations and reduction procedure and analyse the data in terms of the two models.

Table 1. Details of the MUSICOS-94 campaign on γ Dor. The epoch of the Julian day (JD) is 2449600.00; N is the number of spectra obtained.

Site	Observer	JD start	JD end	N
ESO	Lagrange	59.58	59.88	80
ESO	Lagrange	60.52	60.88	113
ESO	Lagrange	62.52	62.87	88
ESO	Foing	63.58	63.88	90
ESO	Foing	64.60	64.88	113
ESO	Foing	65.61	65.87	79
ESO	Foing	66.61	66.90	99
MSSSO	Lawson	67.02	67.09	6
MSSSO	Lawson	67.92	68.05	5
MSSSO	Lawson	68.93	69.04	5
MSSSO	Lawson	70.91	71.13	15
MSSSO	Lawson	71.93	71.98	4
MSSSO	Lawson	72.91	73.13	13
MSSSO	Lawson	73.92	73.92	1
MSSSO	Lawson	74.92	75.19	14
MtJohn	Hearnshaw	72.92	73.08	6
MtJohn	Hearnshaw	74.90	75.00	5
SAAO	Böhm	75.30	75.60	28
SAAO	Böhm	76.31	76.59	25
SAAO	Böhm	77.30	77.60	27
SAAO	Böhm	78.28	78.42	11
SAAO	Böhm	80.29	80.31	3
SAAO	Böhm	81.28	81.29	2
SAAO	Böhm	82.29	82.30	2
SAAO	Böhm	83.29	83.45	5
SAAO	Böhm	85.30	85.30	1

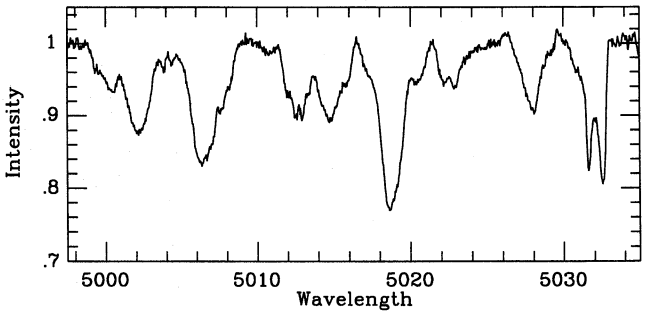

Figure 1. An example of the normalized spectrum of γ Dor obtained at ESO. The feature at 5032 Å is an artefact; the spectrum has not been smoothed.

2 OBSERVATIONS

2.1 Spectroscopy

Spectroscopic data were obtained from four sites during 1994 November: ESO (Chile), Mount Stromlo (Australia), Sutherland (South Africa) and Mount John (New Zealand). The projected rotational velocity of γ Dor is high ($v \sin i = 50$ km s^{-1}), which means that it is impossible to find a totally unblended spectral line. The most suitable line is probably that of Fe II at λ5018.450 Å or possibly Mg I at λ5183.619 Å. Instructions were given to ensure that the λ5018.450 Fe II line was observed whenever possible. The time-coverage at the various sites is shown in Table 1.

The spectra from ESO were obtained using the Coudé Echelle Spectrometer (CES) fed by the 1.4-m CAT. The detector was CCD No.9, a 1024 × 640 thinned back-illuminated RCA-type CCD. The readout noise was about 25 e$^-$ (2 pixel on-line horizontal binning). The grating efficiency was about 97 per cent of maximum; the projected slit width was 48 μm. Only one order was observed with spectral coverage 4998 – 5035 Å and a sampling of 0.033 Å pixel^{-1}. The exposure times were in the range 3 – 5 min, producing well-exposed spectra near the saturation limit. The resolving power was $R = 40\,000$. A Th-Ar lamp was used for wavelength calibration. An example of the spectrum, normalized to the continuum (estimated by eye), is shown in Fig. 1.

The Mt Stromlo and Siding Springs Observatories (MSSSO) spectra were obtained with the coudé echelle on the 1.9-m telescope. The echelle grating has 79 line mm^{-1} with the cross-disperser blazed at 5000 Å. The detector was a 2048 × 2048 Tek CCD with gain of 2 e$^-$ ADU^{-1} and readout

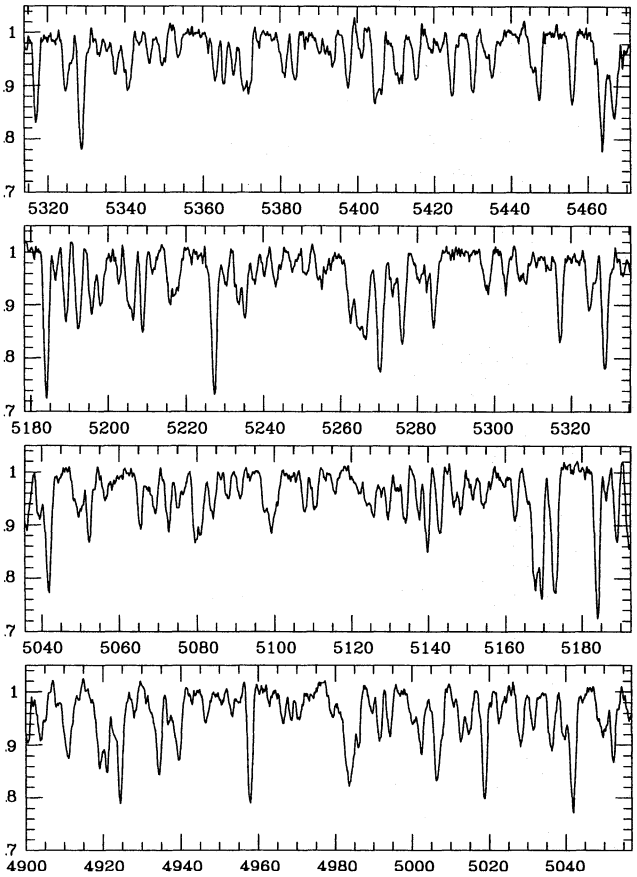

Figure 2. An example of the normalized spectrum of γ Dor obtained from several echelle orders at MSSSO. Spectra from SAAO look almost identical. A running mean box filter with a full width of seven pixels has been applied.

noise of about 2600 e^- (no on-chip binning). The slit width was 200 μm (0.8 arcsec on the sky or 2 pixels on the detector). The pixel size was about 25 μm and resolving power $R \approx 60\,000$. A Th-Ar lamp was used for wavelength calibration. The full spectral range of each order was covered. Each order covers about 87 Å (0.043 Å $pixel^{-1}$) and overlaps with neighbouring orders. An example of a spectrum obtained from 12 orders in the best-exposed range (4900 – 5500 Å) is shown in Fig. 2.

The South African Astronomical Observatory (SAAO) spectra were obtained with the MUSICOS spectrograph attached to the 1.9-m telescope at Sutherland. Details of the instrumentation can be found in Baudrand & Böhm (1992). The detector was a 1024 × 1024 Tek CCD with gain of 2 e^- ADU^{-1} and readout noise of 46 e^- (no on-line binning). The pixel size was 24 μm; the spectral resolution $R = 31\,000$. The full spectral range of each order was covered; neighbouring orders overlap in wavelength. Each order covered about 76 Å (0.074 Å $pixel^{-1}$). The resulting spectra are very similar to those obtained at MSSSO (Fig. 2). A Th-Ar calibration lamp was used.

Spectra from Mt John University Observatory were obtained using the 1.0-m McLellan reflector and a Thomson TH 7882 CDA CCD as detector. This chip has 384 × 576 pixels of dimension 23 μm. The slit width was 100 μm, corresponding to 2.0 arcsec on the sky and giving a wavelength resolution of about 0.2 Å and a resolving power $R = 25\,000$. Details of the spectrograph are given in Hearnshaw (1977) and of the CCD detector system in Tobin (1992). These spectra have lower signal-to-noise ratio than the others and a running mean box filter with full width of 15 pixels was applied. Neighbouring orders do not overlap, so it is not possible to construct a continuous spectrum as was done for the Mt Stromlo and SAAO data. The Mt John data were consequently used only to study the λ5018.450-Å line of Fe II and to monitor possible rapid changes in this and other spectral regions.

2.2 Photometry

Strömgren *uvby* photometry was obtained by L. Balona during the last two weeks of 1994 November (simultaneously with the MUSICOS run at Sutherland) using the single-channel photometer attached to the 0.5-m reflector at Sutherland. During this period, K. Krisciunas obtained Johnson *V* photometry from CTIO using the 0.6-m Lowell reflector. The weather was very good from both sites: 12 out of 14 nights were completely or partly photometric at Sutherland, while all 10 nights were photometric at CTIO. A total of 132 *uvby* and 245 *V* observations were obtained. The coverage was 10 – 18 observations per night at Sutherland and 20 – 30 observations per night at CTIO. In both cases a neutral density filter had to be used to avoid saturating the photomultiplier. The nearby F-type stars HR 1291 and HR 1365 were used as local comparison stars. Observations of these two stars flanked each observation of γ Dor.

The spectroscopic and photometric data used in this paper can be obtained by examining the World Wide Web home page of the SAAO (`www.saao.ac.za`).

3 SPECTROSCOPIC REDUCTIONS

Reductions of the Mt John data were made using the `MIDAS` software package. All other data were reduced using `SPEC1` (single-order spectra) and `SPEC2` (multi-order echelle spectra). These programs were written in `FORTRAN` by L. Balona. The programs require, for each night, a list of files of three types: flatfield, arc and object frames. A few object frames are co-added and used to define the ridge line of the spectrum as a function of (X, Y) position on the CCD. The flatfield frames can also be used for this purpose. A certain number of pixels on either side of the ridge line are used to define the extent of the spectrum perpendicular to the dispersion axis (the *X*-axis). These were chosen so as to include practically all the light from the star. A one-dimensional spectrum is formed by adding the pixels along the *Y* direction inside the strip for a given *X* and subtracting the background for this value of *X*. The background is obtained from two strips on either side of the ridge line and sufficiently distant from it as to exclude any starlight. The two strips are added and a running mean applied to define the background as a function of *X*.

The flatfield spectrum is obtained by co-adding all the flatfield frames (excluding those with saturated pixels) and extracting a strip coincident with the ridge line of the stellar spectrum and of the same width. The pixels along the *Y* direction inside the strip are added and the background subtracted to form a one-dimensional spectrum. The resulting flatfield

spectrum is normalized to unit mean and applied to the object spectra.

The arc frames are co-added and a strip coincident with the ridge line of the stellar spectrum, and of the same width, is extracted. This is converted to a one-dimensional spectrum and the background subtracted as described above. Finally, the flatfield correction is applied. The arc lines are fitted by Gaussians using non-linear least squares. This gives precise X positions, which, together with the laboratory wavelengths, are used to calibrate wavelength as a function of X. The arc lines are identified automatically by supplying the approximate wavelengths at two points on the spectrum as well as a list of wavelengths for the fitted lines. This information is contained in the configuration file. A polynomial of second order was found sufficient to fit the calibration curve with a precision of 0.02 – 0.05 Å rms. The output of SPEC1 is a list of ASCII files, one for each object frame, giving intensity versus wavelength.

SPEC2 works in the same way as SPEC1, but on as many orders as desired. As input, the approximate Y positions of the centre of each order are required. Output is a binary file containing the intensity versus wavelength of each order. Subsequent programs read these data and calculate the required intensity factors to match the orders (using the wavelength overlap between orders). Spikes are removed in the process to produce a continuous spectrum covering many orders. Finally, the continuum is estimated by eye and fitted to several points using a spline curve. This is used to normalize the spectrum. For consistency, the continuum points were chosen to be at the same wavelengths for all spectra. The Mt Stromlo spectra suffer from a misaligned flatfield, which produces a rather bumpy continuum for each order when the flatfield is applied. The normalization technique just described was successful in correcting this problem. For both the Mt Stromlo and SAAO data we applied a box running mean filter with total width of seven pixels to remove excess noise (though the unsmoothed spectra could be used).

4 PERIOD ANALYSIS

The periodogram of the combined SAAO y and CTIO V photometry is shown in Fig. 3. The time span of 13 d is not sufficient to resolve the two closely spaced frequencies. The single peak at $f = 1.342$ d^{-1} is a mean of $f_1 = 1.32098$ and $f_2 = 1.36354$ d^{-1}. If f_1 is fitted to the data, a periodogram of the residuals has the strongest peak at 1.387 d^{-1}. Conversely, if f_2 is fitted and removed from the data, the strongest peak in the periodogram is at 1.303 d^{-1}. Because the total duration of the observations is too short to resolve f_1 and f_2, it is not possible to obtain accurate values of the frequencies. Nevertheless, the fact that prewhitening by the known value of f_1 produces a peak close to f_2, and vice versa, shows that the two frequencies are still present.

Since f_1 and f_2 are still present, it is reasonable to assume that the frequencies have remained unchanged over the last few years. To test this, we show in Table 2 the amplitudes and phases for individual seasons using $f_1 = 1.32098$ and $f_2 = 1.36354$ d^{-1} (the third frequency, f_4, is discussed below). It can be seen that the phases over the five years do not differ significantly from the mean, in spite of the small formal errors (these do not take into account the distribution of the observations). The maximum deviation in phase is 0.09 periods for f_1 and 0.06 periods for f_2, while the standard deviation is about 0.03 periods in both cases. The low amplitude during the 1993 season is particularly striking.

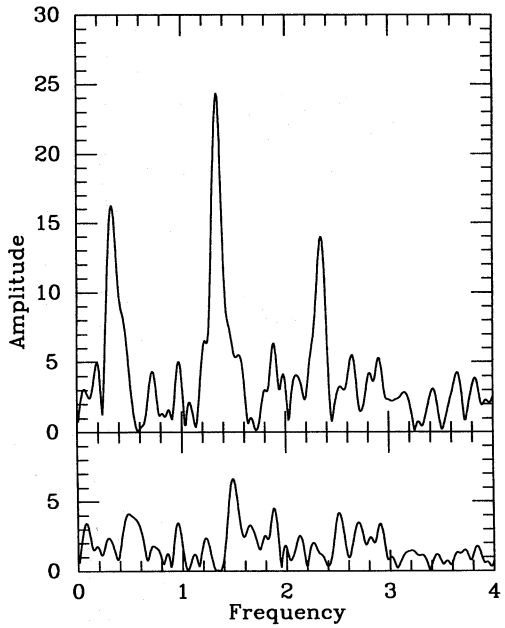

Figure 3. Periodogram of the combined SAAO y and CTIO V data of γ Dor (top panel) and the periodogram after removal of the two principal components, f_1 and f_2 (bottom panel). Amplitude is in mmag, frequency in cycle d^{-1}.

Fig. 3 also shows the periodogram of the 1994 November y and V data after removing the two periodic components. It is clear that a third frequency at $f = 1.4888$ d^{-1} is present. This was strongly suspected by Balona et al. (1994b) who obtained $f_4 = 1.475$ d^{-1}, $A_4 = 7.4$ mmag. This third frequency, f_4, is therefore confirmed. Table 2 shows that the amplitude of this component was below the detectable threshold (about 3 mmag) prior to 1993. A periodogram of the combined 1993 and 1994 seasons gives a best estimate of $f_4 = 1.47447(\pm 5)$ d^{-1}. Table 3 lists the amplitudes and phases of the three periodic components of the V and Strömgren colour indices for the combined 1993 and 1994 seasons. This gives the best estimate of the phases for 1994. However, the amplitudes of f_1 and f_2 for 1994 should probably be taken from Table 2, since they were particularly low in 1993.

5 RADIAL VELOCITY

The radial velocity is determined from the displacement of a spectral line from its laboratory wavelength. If the line is symmetric, the displacement is uniquely defined, since the centroid, median and mode coincide. If it is not symmetric, problems arise as to what is used in defining the displacement. This is always a problem in pulsating stars, since the lines are almost always skew. The cross-correlation technique is often used to determine the radial velocity, but this does not get around the problem which is now transferred to defining the position of the (possibly asymmetric) correlation function. In this paper we will adopt the *centroid* (the first moment of

Table 2. Amplitudes (A_j) and phases (ϕ_j) of a three-component Fourier fit to the V data between 1989 and 1994. The frequencies are $f_1 = 1.32098$, $f_2 = 1.36354$, $f_4 = 1.47447$ d^{-1} and the epoch is JD 2449000. Semi-amplitudes are in millimags; phases are in fractions of a period. The JD is with respect to 2440000; N is the number of observations.

JD	N	A_1	ϕ_1	A_2	ϕ_2	A_4	ϕ_4
7838 - 7970	175	16.8 ± 1.0	0.03 ± 0.01	12.9 ± 1.0	0.26 ± 0.02	3.0 ± 1.0	0.56 ± 0.05
8185 - 8327	107	12.8 ± 1.2	0.04 ± 0.02	15.6 ± 1.2	0.27 ± 0.01	2.6 ± 1.2	0.39 ± 0.08
8993 - 9005	278	16.3 ± 1.2	0.09 ± 0.01	19.5 ± 1.5	0.31 ± 0.01	2.6 ± 0.3	0.26 ± 0.03
9326 - 9406	331	6.8 ± 0.7	0.98 ± 0.02	9.5 ± 0.7	0.19 ± 0.01	5.9 ± 0.6	0.91 ± 0.02
9672 - 9685	377	14.9 ± 0.7	0.92 ± 0.01	13.4 ± 0.7	0.21 ± 0.08	7.2 ± 0.5	0.14 ± 0.01

Table 3. Amplitudes (A_j) and phases (ϕ_j) of a three-component Fourier fit to the radial velocity, V_r, and V, $b-y$, c_1 and $u-b$ (1993 and 1994 seasons). The frequencies are $f_1 = 1.32098$, $f_2 = 1.36354$, $f_4 = 1.47447$ d^{-1} and the epoch is JD 2449000. Semi-amplitudes are in km s^{-1} for V_r and in millimags for the photometry; phases are in fractions of a period.

	A_1	ϕ_1	A_2	ϕ_2	A_4	ϕ_4
V_r	0.3 ± 0.1	0.02 ± 0.05	1.3 ± 0.1	0.64 ± 0.01	0.6 ± 0.1	0.47 ± 0.02
V	11.6 ± 0.5	0.97 ± 0.01	13.5 ± 0.5	0.21 ± 0.01	6.7 ± 0.5	0.14 ± 0.01
$b-y$	3.9 ± 0.5	0.02 ± 0.02	2.5 ± 0.5	0.32 ± 0.03	2.1 ± 0.4	0.21 ± 0.03
c_1	11.7 ± 0.8	0.53 ± 0.01	7.9 ± 0.8	0.80 ± 0.02	2.5 ± 0.7	0.63 ± 0.05
$u-b$	5.8 ± 0.7	0.55 ± 0.02	4.1 ± 0.7	0.85 ± 0.03	1.7 ± 0.6	0.60 ± 0.06

the line profile) as the measure of displacement because it is easy to calculate and because it is used in theoretical work on pulsating stars.

In the case of γ Dor, the most accurate measurement of radial velocity is obtained by making use of the echelle spectra from MSSSO and SAAO. We used the first spectrum obtained at SAAO as the master and determined the radial velocity by cross-correlation with this spectrum. The periodogram of the radial velocities (Fig. 4) shows a peak at $f = 1.365 \pm 0.002$ d^{-1}, very close to f_2. Although the data sampling is not sufficient to resolve the three frequencies in the periodogram, numerical tests show that the correct amplitudes are recovered if the frequencies are given. Since we already know the frequencies with high accuracy, Fourier decomposition of the radial velocities allows the amplitudes and phases to be determined: these are shown in Table 3. The light, colour and radial velocities for each of the three periodic components are shown in Fig. 5. The standard deviation of one observation for the radial velocity is found to be 0.68 km s^{-1}.

An important result of these observations is the ratios of radial velocity to light amplitude for the three periodic components. Note that the light amplitudes for the f_1 and f_2 components are comparable, but that the radial velocity amplitude of f_1 is very much smaller than that of f_2. It is not easy to understand how two starspots could produce such different radial velocity to light amplitude ratios. On the other hand, NRP can account for this difference if the two components belong to different modes. The ratios of radial velocity to light amplitude for f_2 and f_4 are nearly the same, indicating that (ℓ, m) for these two components could be the same (as indeed they are – see below). Note also that, in f_2, radial velocity maximum occurs near light maximum. This again is not consistent with the starspot model, where you would expect radial velocity maximum to occur when the spot is receding, i.e. a quarter of a period after minimum light for a dark spot (or a quarter of a period after maximum light for a bright spot).

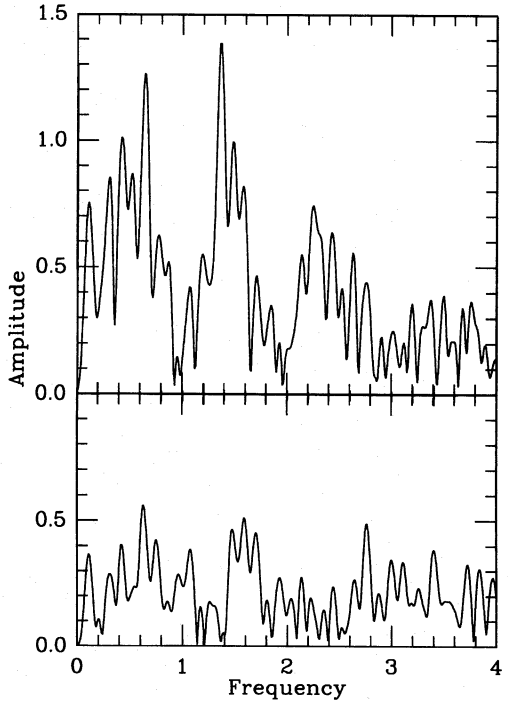

Figure 4. Periodogram of the radial velocities obtained by cross-correlation of the SAAO and MSSSO multi-order echelle data (top panel) and after removing the frequency $f = 1.365$ d^{-1} (bottom panel). The amplitude is in km s^{-1}, the frequency in cycle d^{-1}.

6 THE MOMENTS

To determine the pulsation modes for each of the three periods in γ Dor, we need to measure the first few moments of a particular spectral line as a function of time. As already mentioned, the λ5018.450-Å line of Fe II was chosen because it is strong and relatively unblended. The procedure for obtaining

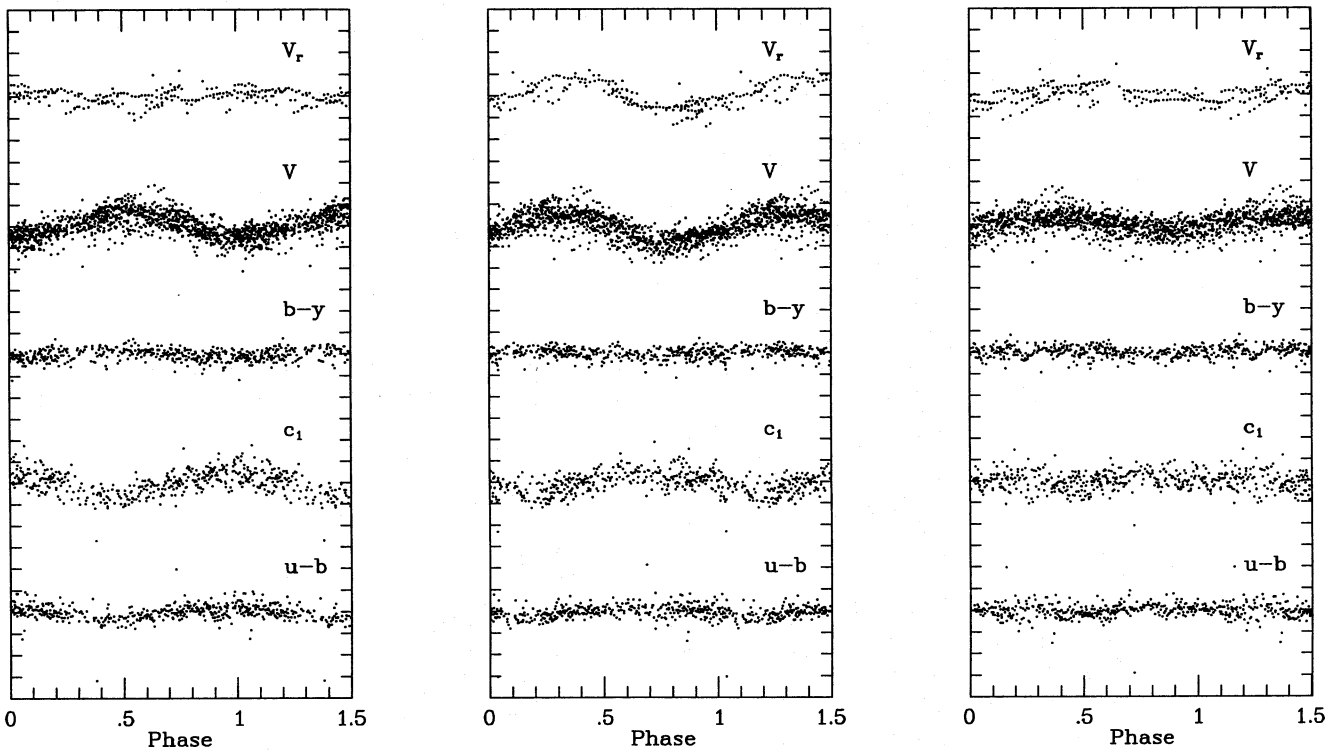

Figure 5. The radial velocity, light and colour curves for the periodic component $f_1 = 1.32098$ d^{-1} (left), $f_2 = 1.36354$ d^{-1} (middle) and $f_4 = 1.47447$ d^{-1} (right). The epoch of phase zero is JD 2449000. Tick marks are spaced at intervals of 2 km s^{-1} for the radial velocity curve and 0.02 mag for the light and colour curves.

the moments has been automated in a program called DoSpec (written by L. Balona).

In general, DoSpec looks for spectral absorption lines with central depth greater than a certain threshold, fits them by Gaussians, and removes them from the spectrum. The threshold is lowered and the procedure repeated until a certain level is reached. DoSpec then adds each fitted line back to the spectrum, calculates the moments, and removes the line again. In this way moments are calculated which are relatively free of the effects of neighbouring lines. The output is a file listing all lines in the spectrum and their first seven moments (moments 2 – 6 are calculated relative to the centroid). The moment of order zero is just the equivalent width (EW), the first moment is the centroid (from which the radial velocity can be calculated), the second moment is the rms width of the line, etc.

DoSpec was applied to the neighbourhood of the λ5018 line using all available spectra (ESO, Mt Stromlo, SAAO and Mt John). The periodogram of the radial velocity of this line from the combined data is rather puzzling as the strongest peak is at $f = 0.734$ d^{-1}. This is different from any frequency so far identified, though it is rather close to $f_4/2$. However, if only the SAAO and Mt Stromlo data are used, the periodogram is quite different, having a peak at $f = 1.359$ d^{-1}. This is clearly f_2, identified above from the radial velocity obtained by cross-correlation. The periodogram from the ESO and Mt John data alone shows a peak at $f = 0.728$ d^{-1}. These periodograms are shown in Fig. 6.

We do not understand why the ESO data do not show any power at or near $f = 1.36$ d^{-1}. A phase diagram of the first moment (m_1) of the ESO data phased with f_1, and f_4 (Fig. 7) shows reasonable agreement with the SAAO & MSSSO curves (see Fig. 8). However, for f_2 the curve seems to be of the double-wave type with a minimum at about phase 0.9 and another minimum at phase 0.4, where the SAAO & MSSSO data show a maximum. The minimum at phase 0.4 arises almost entirely from data for one night (JD 2449664). There is no reason to suspect an instrumental cause for this behaviour, but unfortunately we do not have photometry taken at about the time when the double-wave form developed for f_2. The star is known to display irregular excursions in light from time to time (Balona et al. 1994a). It is possible that such an event may be responsible for the minimum where a maximum is expected, but this cannot be confirmed. One should also take into account the fact the ESO data are rather poorly sampled, several nights having similar mean phase for f_1 or f_2. In view of this problem, we decided it would be better to use the SAAO & MSSSO data only in determining the modes.

7 MODE IDENTIFICATION

Since the phase relationship between the light and radial velocity variations rules out the starspot hypothesis, and since we cannot think of any model invoking orbital motion that may account for the variations, it is safe to assume that NRP is the most probable explanation. However, we need to prove that the parameters required for NRP are physically realistic. To do this, we need to identify the modes of oscillation and determine these parameters.

Any arbitrary distribution can be represented by specifying its moments. The greater the number of moments, the

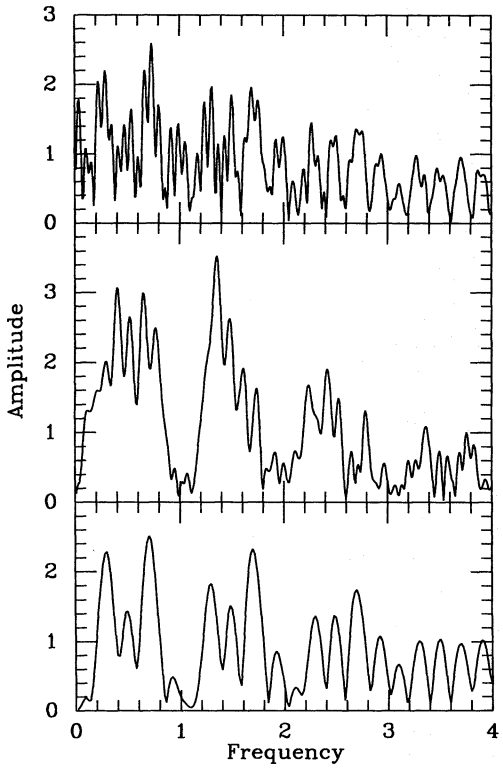

Figure 6. Periodogram of the first moment of the λ5018.450-Å line of Fe II. Top panel – all available data; middle panel – MSSSO and SAAO echelle data; bottom panel – ESO and Mt John data. The amplitude is in km s^{-1}, the frequency in cycle d^{-1}.

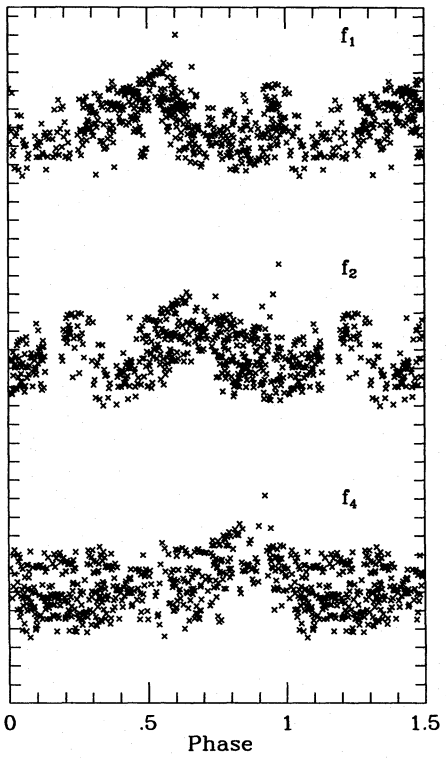

Figure 7. Phase variation of the first moment of the Fe II line λ5018.450 Å from the ESO data for the three periodic components. The epoch of phase zero is JD 244 9000. Tick marks are spaced at intervals of km s^{-1}.

more accurate is the representation. During pulsation, the line profile will vary and so will its moments. For example, in γ Dor the moments will vary with the three frequencies, f_1, f_2 and f_4. The amplitude and phase of a particular moment that belongs to one of the three oscillations can be calculated by fitting a multiperiodic Fourier curve. For a particular angle of inclination, i, and a given mode, (ℓ, m), the amplitudes and phases of the first few moments can be fitted to the predicted ones, and the pulsation parameters obtained by least squares. In general, the fit will be poor unless the chosen values of i, ℓ and m are close to the true values. In this way, the most likely values of i, ℓ and m can be estimated.

This method of mode estimation was developed by Balona (1986a,b, 1987). It uses the algorithms described in Balona (1987) and assumes that the pulsation velocity amplitude is much smaller than the projected rotational velocity. This is certainly true in γ Dor where the radial velocity semi-amplitude is less than 2 km s^{-1}, whereas $v \sin i = 50$ km s^{-1}. The algorithm uses a first-order expansion in the ratio Ω/ω (Ω being the frequency of rotation and ω the frequency of pulsation). The eigenfunctions of a rotating, pulsating star are well described by pure spherical harmonics only when this ratio is small. This is not the case in γ Dor. In Balona et al. (1994a), the stellar radius is found to be $R = 1.32$ $R_\odot$. Using the value $v \sin i = 50$ km s^{-1} gives a rotation period $P_{\rm rot} < 1.34$ d. Therefore $\Omega/\omega > 0.55$. For such a large ratio, departures of the eigenfunctions from pure spherical harmonics are bound to be significant and we do not expect a very good fit on the basis of a first-order expansion. Spheroidal modes with different values of (ℓ, m) are mixed in, and so are toroidal modes. These additional components will have lower amplitudes, so we can expect the method to identify the dominant spherical harmonic mode (ℓ, m).

Aerts & Krisciunas (1996) apply a similar method in their analysis of 9 Aur. However, the rotational velocity of this star is rather low and the velocity variations larger than in γ Dor. The approximation discussed above is probably not a good one for this star, and a different algorithm was used. Owing to the low rotational velocity, the algorithm is incapable of distinguishing between prograde ($m < 0$) and retrograde ($m > 0$) modes.

We use the Fe II line λ5018.450 Å to probe the pulsation mode. It may be possible to use more than one line to improve the signal-to-noise ratio. In fact, Aerts & Krisciunas (1996) use the profile obtained from the cross-correlation of the spectrum with a mask in the CORAVEL instrument for this purpose. We have not tested the reliability of this procedure. First, we calculate the centroid (first moment) of the line profile, which gives the radial velocity. Then we calculate higher-order moments with respect to the centroid as origin. The moments that are actually required are those with respect to the centre of mass of the star. This means that we need to determine the mean radial velocity, and then re-calculate all the higher order moments with respect to this velocity (rather than the centroid). Transformation of the origin of the moments from the centroid to the centre-of-mass velocity is easily accomplished using a polynomial expansion. Using only the MSSSO and SAAO data, the mean radial velocity is $< m_1 >= 22.4 \pm 0.2$ km s^{-1}; the standard deviation of one observation being 2.3 km s^{-1}. The standard deviation is

larger than in the cross-correlation technique because only one line is used. A few published radial velocity measurements are available (Abt & Biggs 1972). These range from 20 to 27 km s^{-1}, in good agreement with the value obtained here from the Fe II line.

In Fig. 8, we show the variation of the equivalent width (EW) and the first four moments of the Fe II line λ5018.450 Å phased with f_1, f_2 and f_4 for the combined MSSSO and SAAO data. The amplitudes and phases are shown in Table 4. We have fitted the data with all three periodicities because these periodicities are present in the light curve. It might be argued that the only period that is definitely present in the radial velocities is f_2. It is certainly true that f_2 has the highest amplitude, but this could be merely a result of the particular non-radial mode favouring the first moment as opposed to other moments. The amplitude of the radial velocities (and other moments) places a constraint on the mode identification even if it is close to zero. It is therefore necessary to determine the amplitudes and phases of the moments of all three periodicities if one is to understand how the light variations are produced.

The mean equivalent width is $< EW >= 0.369 \pm 0.001$ Å (the standard deviation for one observation is 0.015 Å). It is surprising to find that there is significant variation of the EW when phased with f_1, but not with f_2 or f_4. For the f_1 component, the EW reaches a maximum at about the time of maximum c_1 colour, i.e. slightly before maximum light. On the other hand, there is no significant variation with f_2 even though the light and colour amplitude is almost the same as f_1.

Only a few moments show significant phase variation, which is not surprising in view of the low radial velocity amplitude of the star. This means that mode identification will be indeterminate unless we use the most significant variations and employ as many constraints as possible. In the case of γ Dor we need to consider how we can constrain the pulsational parameters. NRP generates a variable temperature distribution on the photosphere which distorts the line profile owing to rotation of the star. This effect can be quantified as a fictitious velocity field, v_f. It is fictitious because it is not generated by the variation of displacement during pulsation. Instead, the spatial variation of temperature across the photosphere caused by non-radial pulsation, in combination with rotation of the star, adds or removes flux from the line profile. The net result is a change in the radial velocity as measured by the centroid or line minimum. It plays an important role only if rotation is reasonably rapid. Very crudely, the amplitude of the velocity generated by this effect is approximately given by the product of the relative luminosity variation and the projected rotational velocity. In γ Dor, the semi-amplitude of the light variation is about 0.01 mag and $v \sin i = 50$ km s^{-1}, so we expect $v_f \approx 0.5$ km s^{-1}. This is comparable to the observed radial velocity semi-amplitude and cannot be neglected.

The other velocity fields are v_r – the pulsational velocity in the vertical direction and v_h – the pulsational velocity in the horizontal direction. For each of these three velocity fields, the amplitude and phase need to be determined, giving six free parameters for a given i, ℓ and m. We know that v_r must be small compared with v_h because the three modes must all be g modes. The ratio

$$\frac{v_h}{v_r} \approx \frac{4\pi^2 f^2 R^3}{GM}$$

is approximately 36 for γ Dor. Hence we may safely ignore v_r and limit the solutions to v_f and v_h only, resulting in four free parameters. A further constraint can be imposed: $v_f < v \sin i$, since larger values imply a relative flux variation greater than unity.

To first order, the horizontal velocity component, v_h, will not contribute to the light variation since there is no geometric distortion. All the light variation arises from the temperature variation during pulsation (v_f). On the other hand, v_h will certainly contribute to the distortion of the line profile. The amplitude and phase of the light curve are determined only by v_f, but the amplitude and phase of the radial velocity curve depend on v_h as well as v_f. This allows for a different phase relationship between the two curves from that predicted by the spot model.

The light curve and the radial velocity curve can therefore be used to determine v_f and v_h for any i, ℓ and m, but at least one more moment is required to produce a discriminant. In principle, a solution can be obtained using the amplitudes and phases of the light curve and the first two moments only. However, there is information in the third and higher moments which should be used to constrain the solution. It is clear, however, that the higher order moments should be given less weight because they have larger uncertainties. The weights to be assigned to a particular moment can be determined from the standard error of its amplitude and phase (easily calculated from the Fourier fit). The equations of condition in the algorithm have dimensions of velocity, since each equation is divided by $(v \sin i)^{n-1}$ for the nth moment. Hence the appropriate weight is obtained by dividing the standard error of the moment by this quantity. This results in the following standard deviations being assigned to each moment: light curve 1.00; first moment 2.09; second moment 2.73; third moment 6.82; fourth moment 11.84 km s^{-1}.

The zero-points of the second and fourth moments of the line profile are sufficient to determine the projected rotational velocity and the rms line width (W_i) of the intrinsic profile. W_i includes a contribution to the intrinsic line width owing to the finite resolution of the instruments (the difference in resolving power of the SAAO and MSSSO spectrographs is equivalent to about 5 km s^{-1}). In principle, it is possible to determine W_i for the two instruments, but it is unlikely that this difference would be significant. The zero-points of the second and fourth moments are $m_2 = 1897 \pm 14$ and $m_4 = (10.54 \pm 0.16) \times 10^6$ in units of km s^{-1} to the respective powers. Using a limb darkening value of $u = 0.5$, appropriate for an early F-type star in the visible region, we find $v \sin i = 48$ km s^{-1} and $W_i = 37$ km s^{-1}. The value of $v \sin i$ agrees well with that of Slettebak et al. (1975). These values are used to deconvolve the moments to the values they would have had in the limit of zero intrinsic width as described in Balona (1986a,b, 1987).

Using these values, we calculated the discriminant, σ, for a choice of mode (ℓ, m) as a function of angle of inclination, i, using the weighted light curve and first four moments. In this calculation, we adopted a radius $R = 1.32$ R$_\odot$, a limb darkening coefficient $u = 0.50$, and the Ledoux rotational splitting coefficient, $C = 0.1$ (a typical value; the exact value is unimportant). The computation included all modes up to $\ell = 4$. The discriminant is plotted against angle of inclination in Fig. 9 for the three modes.

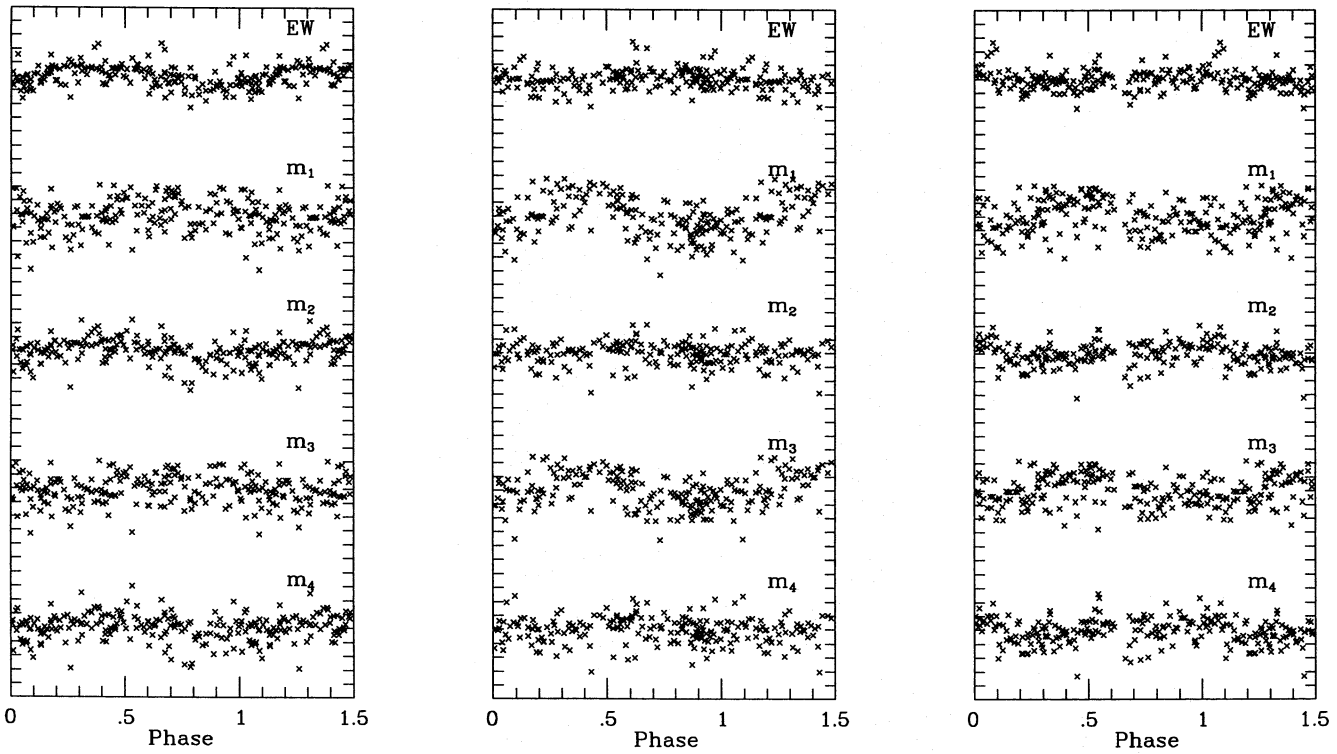

Figure 8. Phase variation of the equivalent width (EW) and the first four moments ($m_0 - m_4$) of the Fe II line λ5018.450 Å phased with f_1 (left), f_2 (middle) and f_4 (right). The epoch of phase zero is JD 244 9000. Tick marks are spaced at intervals of 0.02 Å for EW and 2 km s^{-1} for m_1. The other moments are plotted on an arbitrary scale.

Table 4. Amplitudes (A_j) and phases (ϕ_j) of a three-component Fourier fit to the EW and first four moments of the Fe II line λ5018.450 Å for the combined MSSSO and SAAO data. The frequencies are $f_1 = 1.320\,98$, $f_2 = 1.363\,54$, $f_4 = 1.474\,47$ d^{-1} and the epoch is JD 244 9000. Semi-amplitudes are in mÅ for the EW, in km s^{-1} for m_1 and in powers of km s^{-1} for the other moments ($m_2 \times 10^2, m_3 \times 10^4, m_4 \times 10^5$). Phases are in periods.

	A_1	ϕ_1	A_2	ϕ_2	A_4	ϕ_4
EW	11.4 ± 2.2	0.60 ± 0.03	5.9 ± 2.6	0.24 ± 0.06	5.0 ± 1.8	0.04 ± 0.06
m_1	1.0 ± 0.3	0.30 ± 0.06	2.3 ± 0.4	0.61 ± 0.03	1.4 ± 0.3	0.53 ± 0.03
m_2	1.1 ± 0.3	0.59 ± 0.04	0.4 ± 0.3	0.38 ± 0.12	0.6 ± 0.2	0.12 ± 0.05
m_3	0.7 ± 0.3	0.27 ± 0.07	1.9 ± 0.3	0.62 ± 0.03	1.2 ± 0.3	0.54 ± 0.03
m_4	9.0 ± 3.0	0.58 ± 0.05	4.8 ± 3.0	0.39 ± 0.11	6.1 ± 2.4	0.19 ± 0.06

Since the angle of inclination must be the same, f_2 constrains $i > 50°$. The (3, 1) mode leads to a light amplitude which is too low except over a very small range near $i = 77°$. Therefore, we can identify f_2 as either (2, –1) or (1, 1). Both give realistic pulsation parameters and good agreement with the light amplitude for an inclination $65° < i < 80°$, but the (2, –1) mode does not match the phase of the light curve very well. With this limit on the angle of inclination, we find that f_1 can only be (3, 3). This also gives realistic pulsation parameters and good agreement with the light curve. Finally, we find (1, 1) as the best estimate for f_4, since (2, 0) and (2, –1) produce light amplitudes which are twice as high as observed.

Another way of imposing the constraint that the inclination angle for all three modes must be the same is to calculate the sum of the weighted discriminant at a particular value of i for the three modes for all values of (ℓ, m). When the minimum of this sum is plotted against angle of inclination, an indication of the uniqueness of the solution can be ascertained. This is shown in Fig. 10 where we have chosen weights of unity for f_1 and f_2, and a weight of 0.25 for the less significant f_4. There is no solution for $i < 7°$ because this would imply an equatorial velocity larger than the breakup velocity. The variance for $45° < i < 63°$ is too large to be plotted. The figure shows that the best solution is found for $i > 63°$. As mentioned above, the identifications for this range are (3, 3) for f_1, (2, –1) or (1, 1) for f_2 and (1, 1) for f_4.

On the basis of these data, we conclude that the angle of inclination of γ Dor is probably $i \approx 70°$, and that the best estimates of the values of (ℓ, m) for the three oscillations are: (3, 3) for f_1, (1, 1) for f_2 and for f_4. Table 5 gives the pulsational parameters for this angle of inclination.

Table 5. Pulsation parameters for the most probable mode identifications, (ℓ, m), for the three oscillations in γ Dor. The angle of inclination is assumed to be $i = 70°$.

	(ℓ, m)	σ	v_f	$\phi(v_f)$	v_h	$\phi(v_h)$	$A(V)$	$\phi(V)$	$A(V_r)$	$\phi(V_r)$
f_1	(3, 3)	1.64	15.2	0.13	8.4	0.09	0.006	0.13	1.00	0.31
f_2	(1, 1)	1.77	3.2	0.25	12.8	0.35	0.016	0.25	2.35	0.61
f_4	(1, 1)	2.32	1.6	0.26	8.5	0.26	0.008	0.26	1.54	0.51

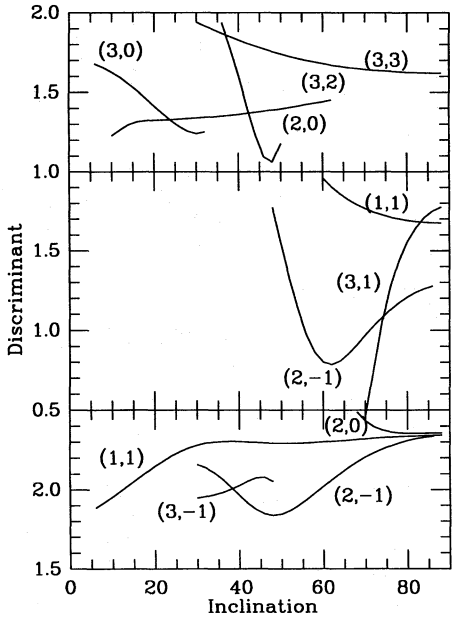

Figure 9. Discriminant (arbitrary units) as a function of angle of inclination (in degrees) for various modes (ℓ, m). Top panel: $f_1 = 1.32098\ \mathrm{d}^{-1}$; middle panel: $f_2 = 1.36354\ \mathrm{d}^{-1}$; bottom panel: $f_4 = 1.47447\ \mathrm{d}^{-1}$.

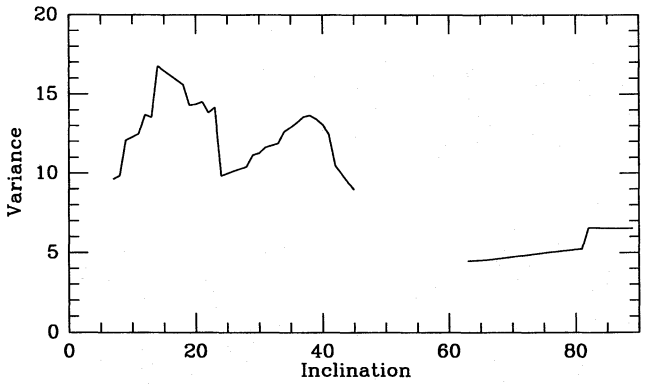

Figure 10. The minimum sum of the discriminant variance over all three modes is shown as a function of angle of inclination (in degrees). The best solution is found for $63° < i < 80°$.

8 DISCUSSION

One of the most puzzling aspects of γ Dor is the sudden appearance, from time to time, of isolated absorption or emission features (Balona et al. 1994a). Careful inspection of all the spectra obtained during the MUSICOS-94 campaign has failed to reveal such oddities. The star appears to have a normal early-F spectrum, though broadened by rotation. There is no doubt, however, that the light variations of the star cannot be explained entirely by three periodic components. There is a certain level of non-periodicity which is not yet understood (Balona et al. 1994a,b). The spectroscopic observations during MUSICOS-94 show evidence for this effect on one night (JD 2449664), where the radial velocities are substantially smaller than expected.

Our new photometric observations confirm the existence of a third oscillation, $f_4 = 1.47447\ \mathrm{d}^{-1}$, previously suspected by Balona et al. (1994b). The existence of three frequencies implies substantial differential rotation on the basis of the starspot model. This model also fails to account for the great differences which exist between the radial velocity to light amplitude ratios for the two main oscillations. However, the most serious objection to the starspot model is the fact that for f_2 radial velocity and light maximum coincide in phase. One would expect a 90° phase difference for a starspot. The small radial velocity amplitude also excludes the possibility of a binary companion. We conclude that non-radial pulsation is the only viable explanation for the observations.

From the light curve and first four moments of the line profile of Fe II λ5018.450 Å, we show that γ Dor has a high angle of inclination, probably $i \approx 70°$, and that the three modes may be identified as $f_1 = (3, 3)$, $f_2 = f_4 = (1, 1)$ with fair confidence. The pulsation parameters indicate quite a large value $v_f = 15.2\ \mathrm{km\ s^{-1}}$ for f_1. Now the relative flux amplitude

$$\frac{\Delta F}{F} = \frac{v_f}{v \sin i}$$

which gives $\Delta F/F = 0.32$ for f_1, implying that this mode produces a large temperature variation $\Delta T/T \approx 0.08$. This may account for the significant phase dependence of the equivalent width for this mode, whereas the other modes show little or no phase dependence. The fact that the amplitudes of the colour indices c_1 and $(u-b)$ are larger in this mode is also consistent with the large v_f.

The observation that f_2 dominates the radial velocity variation, but that f_1 does not, though they have similar light amplitudes, is due to the fact that f_1 has a relatively high spherical harmonic degree $\ell = 3$, whereas f_2 has the lower value $\ell = 1$. The averaging effect in the latter case is much less, leading to a larger radial velocity amplitude. On the other hand, the much larger value of v_f for f_1 compensates in the light curve.

It is interesting that all three modes seem to be sectorial retrograde modes. The frequency of pulsation in the co-rotating frame, ν_0, is related to the frequency of pulsation in the observer's frame, ν, by: $\nu_0 = \nu + m\Omega$ where Ω is the frequency of rotation. If $i = 70°$ and $R = 1.32\ \mathrm{R}_\odot$, we find $\Omega = 1.04\ \mathrm{d}^{-1}$ ($P_{\mathrm{rot}} = 0.96$ d). Thus, in the co-rotating frame, the three oscillations have the following frequencies: $f_{10} \approx 4.44$, $f_{20} \approx 2.40$ and $f_{40} \approx 2.51\ \mathrm{d}^{-1}$. f_1 and f_2 are substantially

different and must have quite different radial orders in spite of the fact that they are nearly equal in the inertial frame. On the other hand, f_2 and f_4, which are of the same degree, ℓ, probably have neighbouring radial orders. This information could be used to extract seismological information, but the effect of rotation needs to be taken into account more accurately before this can done.

The success of mode identification in this star is encouraging. The application of the method to other stars might well lead to very interesting results, as in the case of 9 Aur (Krisciunas et al. 1996), but other types of pulsating star may be equally interesting. For example, an intensive campaign on a periodic Be star (and there are many of these that are bright) should result in a definitive test of the NRP/starspot models (Balona 1996). All that would be required is an accurate determination of the radial velocity to light amplitude ratio.

ACKNOWLEDGMENTS

JBH thanks O. K. Petterson for assistance with MIDAS reductions. LAB and WAL thank the Director of MSSSO for telescope time. KK thanks Malcom Smith for Director's Discretionary Time at CTIO, and thanks the Joint Astronomy Centre for observing support.

REFERENCES

Abt H.A., Biggs E.S., 1972, Bibliography of Stellar Radial Velocities. Kitt Peak National Obs., Tucson, USA
Aerts C., 1993, PhD Thesis, Katholieke Univ. Leuven, Belgium
Aerts C., Krisciunas K., 1996, MNRAS, 278, 877
Aumann H.H., 1985, PASP, 97, 885
Balona L.A., 1986a, MNRAS, 219, 111
Balona L.A., 1986b, MNRAS, 220, 647
Balona L.A., 1987, MNRAS, 224, 41
Balona L.A., 1996, MNRAS, in press
Balona L.A., Hearnshaw J.B., Koen C., Collier A., Machi I., Mkhosi M., Steenberg C., 1994a, MNRAS, 267, 103
Balona L.A., Krisciunas K., Cousins A.W.J., 1994b, MNRAS, 270, 905
Baudrand J., Böhm T., 1992, A&A, 259, 711
Hearnshaw J.B., 1977, Proc. Astron. Soc. Aust., 3, 102
Krisciunas K., Handler G., 1995, Inf. Bull. Variable Stars, 4195
Krisciunas K., Griffin R.F., Guinan E.F., Luedeke K.D., McCook G.P., 1995, MNRAS, 273, 662
Mantegazza L., Poretti E., Zerbi F.M., 1994, MNRAS, 270, 439
Slettebak A., Collins D.W., Boyce P.B., White N.M., Perkinson T.D., 1975, ApJS, 29, 137
Tobin W., 1992, South. Stars, 34, 421

This paper has been produced using the Royal Astronomical Society/Blackwell Science LaTeX style file.